6. An Integrated Monitoring and Control System for THOR

H. P. Chou, T. H. Chou and T. L. Chen

ABSTRACT

The paper presents a computerized monitoring and control system for the THOR. The system is used to assist reactor operation and to facilitate data acquisition and teaching for reactor experimental laboratory courses. The design applies digital data processing for neutron detector and area monitor measurements. Signal validation is used to improve signal reliability. Color pictures in the forms of analog meters, strip charts, and bar graphs are displayed for the control room and for off-site as well. Power control is based on the "reactivity constraint" approach for wide range adjustment and on-off logics for narrow range regulation. Algorithms are coded in C language and implemented into a 32-bit microcomputer. Evaluations have shown satisfactory results for operation and teaching needs.

INTRODUCTION

The Tsing Hua Open-pool Reactor (THOR) was built near 1960 and has played an important role in the university's teaching and research activities since then. A THOR improvement program began several years ago; the reactor core was converted from the MTR plate-type fuel into the TRIGA rod-type fuel to upgrade its power level. The neutron detection system was upgraded with wide range fission chambers and modern integrated circuits to improve its sensitivity and reliability. Power maneuver at the THOR is performed using three safety control blades and one regulating blade. The original vacuum tube type power servo system was also replaced with integrated circuit devices.[1] The instrument display panels and the power control scheme, however, remain to be the original analog setup.

Recently, digital signal processing techniques and computer control strategies have a great advance and have successfully applied in many industries; examples can also be found for nuclear research reactors.[2-5] At the mean time, digital data analysis using microcomputers has become a common practice in many laboratory courses. Data acquisition from the conventional analog display panels are often troublesome for students during reactor experiments. The conventional power servo system using the DC differential level comparison technique was designed for narrow range power regulation and was found inconvenient for frequent power maneuvers during the student laboratory practices. Therefore, there is an interest in the development of a computerized monitoring and control system to assist the THOR operation as well as to meet the teaching needs.

Under the limited budget and time constraints, we have proposed to develop a microcomputer based system and concentrate the effort on the display and

control schemes while leave the reactor protection system, transducer systems, and mechanical setups untouched. To minimize hardware change and operation interference, we have the system attached in parallel with the existing ones. For the reactor experiment laboratory course, we would also like the system to run an off-line test mode to provide simulations of power maneuvers and to illustrate the basic reactor operating principles. Following sections present the system architecture, monitoring and control schemes, and performance demonstration.

SYSTEM ARCHITECTURE

Figure 1 illustrates the overall hardware arrangement. A 32-bit microcomputer acts as the control center for data acquisition and distribution. The VGA color monitor and the remote panels are for information display; the hard disk is used for data logging and storage. The electronic circuits are a relatively low-cost board level design using entirely off-the-shelf components. A modular approach is taken to reduce the maintenance effort. The system is designed to interface with the existing reactor power detection system, area radiation system, and control blade moving assemblies. Interfacing with the process signals, such as temperature and flow rate, is not considered for the time being.

The reactor power detection system consists of two wide range fission chambers and associate amplifier modules. Each detector channel provides a linear power signal and a log power signal. The area radiation monitor system has eight monitors distributed in the reactor building for radiation safety. Signal processor are designed to accept these output and feed into an analog digital (A/D) converter. Each signal processor consists of an isolation amplifier and a low pass filter. The low pass filter is a third order Butterworth circuit with the 3 dB frequency at 2 Hz. The A/D converter is a commercial product designed to use with personal computers; there are 16 channels with a 13-bit resolution. The A/D converter circuit board also contains 64 k-byte buffer memory and a co-processor for digital data preprocessing. The position signal of the control blades is generated from an electrical brush coding system. The position reading is a four-digit number with the voltage level of 25 volts and has the least significant number to be 0.01 inch. The position signal processor module contains a decoder circuit and converts the position signals to meet the TTL standards. The TTL digital readings are then feed to the computer through a parallel input/output interface board and to seven-segment LED displays on the THOR control panel.

The motor driver circuit is designed using digital IC components and solid state relays. A zero-voltage turn-on/turn-off circuit, interlocks with limit switches, and detection logics for contradictory commands are used for motor protection. In case of power failures, the relay is open and the control function can be override manually from the control panel.

Information for the remote display panel are transmitted using the RS-422 standards. Four display panels are installed in the remote experimental area and the emergency control center. Each panel is equipped with a single chip microprocessor for signal flow control and can perform self tests. Alarms are provided during high radiation level and over power transients.

MONITORING AND CONTROL SCHEMES

The monitoring and control schemes perform the following tasks:

1. validation of power, radiation, and control blade position measurements;
2. estimation of dynamic period and core reactivity;
3. reactor power control and regulation;
4. information display and man–machine interface.

Figure 2a illustrates the flow chart of the execution sequence. The schemes are coded in Turbo C language and are designed for both on–line and off–line operation.

During on–line operation, reactor power signals are sampled with 100 Hz frequency and the area monitors and control blade positions are scanned every second. Blade control commands are formatted in a 1 Hz square wave with a 50% duty cycle. During off–line operation, the core reactivity is generated from the pre–calibrated control blade worth data. The power and the blade positions are calculated according the point kinetics equations and the average blade traveling speed respectively. Data logging using disk storage and/or printing is user–defined with selectable frequency.

For parameter estimation, the sampled power signal are averaged every 0.5 s to smooth the high frequency quantization error. The smoothed linear power readings are then checked against a predicted value that is exponentially extrapolated from the previous readings. If the difference is beyond a certain amount, say ± 50%, the reading is replaced with the predicted one. The validated linear power readings are then combined with the integer part of the logarithmic power readings to indicate the power level.

The area monitoring readings are checked using the standard deviation of the data in the previous time interval of 100 s. Warnings are issued, if the disagreement lasts for a certain time steps. The control blade position readings are checked for jump failures according to the maximum available motor speed; the faulty reading is replaced with the previous one and a warning is issued.

Estimation of the dynamic period and the core reactivity is based on the smoothed and validated power readings.. The inverse of the dynamic period, defined as the slope of the logarithmic power, is calculated and smoothed by taking the moving average value every four time steps. The core reactivity is calculated according to the inverse point kinetics equation with six delayed neutron groups. In general, the value of the core reactivity is much less than the delayed neutron fraction β. Thus, the prompt jump approximation is considered a reasonable assumption and the reactivity ρ can be expressed as:

$$\frac{\rho(t)}{\beta} = 1 - \frac{S_d}{\beta\, p(t)} \qquad (1)$$

where p(t) is the power reading and S_d is the delayed neutron source. The delayed neutron source can be obtained by integrating the precursor balance equation with the power reading as the known input. Numerically, an integration time interval corresponding to five time constants of each precursor group, $5/\lambda_k$, is taken. The delayed neutron from the shortest half–life group is assumed to be generated promptly and a lead time of approximately 400 s is needed to estimate the population of the longest delayed neutron group.

The power control and regulation scheme determines the control blade motion. The "reactivity constraint" approach [7] is employed for coarse power level adjustment. Basically, the approach compares the time duration expected for the power changing from the current level to the target level with the time duration expected for the reactivity adjusted from the current value to a threshold value. The expected time duration for the power adjustment, T_a, is estimated by linearly extrapolating the logarithmic power based on the current dynamic period τ; i.e.,

$$T_a(t) = \tau(t)\ ln\ \frac{p^f}{p(t)} \qquad (2)$$

where p^f is the target power level. The expected time duration for the reactivity adjustment T_r is estimated by linearly extrapolating the reactivity:

$$T_r(t) = (\ |\rho(t)| - \rho^T \ ) \ / \ \rho_s(t) \qquad (3)$$

where ρ^T is the threshold reactivity and ρ_s is the slope of the reactivity. The threshold reactivity represents the maximum amount of reactivity that can be left in the core so that the neutron power can be reversed by reversing the control blade motion. According to the point kinetics equation with the prompt jump approximation, the threshold reactivity would meet the following constraint:

$$\rho_{sm} \geq | \ \rho_{sf} + \lambda_e \rho^T + \sum_k \beta_k \ (\lambda_k - \lambda_e)| \qquad (4)$$

where λ_e is an effective one group delayed neutron decay constant defined by:

$$\lambda_e = \frac{\sum_k \lambda_k^2 \ \xi_k}{S_d}; \quad \xi_k \text{ stands for the kth group precursor;} \qquad (5)$$

ρ_{sm} denotes the maximum allowable slope of reactivity that can be obtained from control blade motion. The ρ_{sf} denotes the reactivity slope due to temperature feedback effects. In practice, ρ_{sm} is set to according to the calibrated worth curve and the term ρ_{sm} is neglected for staying on the conservative side.

Although the reactivity constraint approach has been demonstrated to be an effective method for power maneuver, the simple on−off control is sufficient for narrow range power regulation from the past experience [1]. Therefore, we modified the existing on−off control circuit with a software and applied when the reactor power falls within 5% of the target value. To avoid excessive control blade motions, we reduce the control frequency to half. Considering the magnitude of the measurement fluctuations, a 2% power dead band is applied. Figure 2b shows the overall flow chart of the control scheme.

DEMONSTRATION

Figure 3 demonstrates the three picture frames designed for the display of the operating conditions. Figure 3a is a duplicate of the remote display panel which shows the operating power and the area radiation levels. Alarms are provided if limits are exceeded and can be acknowledged using a function key. Figure 3b is a condensed display of the main control panel. The picture shows the reactor linear power, logarithmic power and the dynamic period in a form identical to the panel analog meters. The demand power is also marked with a red line in the linear power meter for reference. Control blades are illustrated dynamically in bar graphs. In case that the faulty position readings are detected, the display blinks to warn the operator. Figure 3c is designed to assist the operator for power maneuvering. The history of power, period, and reactivity in the past 200 s is presented to indicate the trend. A demand power is shown on the upper left corner and can be on−line adjusted in units of 10% or 1% of the current power scale using a control (hot) keypads. Function keys are used to switch between the picture frames and the ESC key is used to manual override the build−in control schemes.

The period estimation scheme is on−line tested using transients with the period ranged from 30s to 100s and found to have a mean square error of ± 3%. The reactivity estimation scheme is off−line tested with a given reactivity ranged from 0 to 10 cents and an assumed of power fluctuation of 2%; The results

indicate an error around ± 0.5 cents.

Off-line tests of the control scheme with assumed power fluctuations show overshoots and steady state errors less than 1%. On-line steady state regulation for xenon compensation indicated a steady state error comparable to the power fluctuations ± 1%. Figures 4a and 4b are on-line disturbance tests by suddenly withdrawing and inserting of one main control blade from a critical state. The overshoot is approximately 2% and the steady state error is less than 1%. Figures 5a and 5b illustrates the on-line power adjustment for a factor of three. The result indicates an overshoot less than 2% and a steady state error of 1%.

SUMMARY

A computerized monitoring and control system has been developed for the THOR to assist the operation and to facilitate data acquisition and teaching of laboratory courses. The design considers digital data processing and signal validation to improve signal reliability. Displays are provided for the control room and for off-site information well. The simulated panel meters and operating trend are provided to strengthen the man-machine interface. Evaluations of the control scheme have shown satisfactory results for power regulation, disturbance rejection, and power maneuvering.

ACKNOWLEDGEMENT

The work is under the auspices of the National Science Council of Taiwan, China with contracts NSC78-0413-E007-11 and NSC77-0413-E007-05. The technical support from the technicians of the Reactor Division and the Instrumentation Division, Nuclear Science & Technology Development Center, National Tsing Hua University is gratefully acknowledged.

REFERENCE

[1] Yu Bin, "THOR Automatic Regulating Rod Control System," THOR Internal Report (1984).

[2] H. A. Larson, WW. F. Booty, D. R. Chick, L. J. Christensen, R. J. Forrester, and J. W. Sielinsky, "Installation of Automatic Control at Experimental Breeder Reactor II," **Nucl. Technol., 70,** 167 (1985).

[3] W. P. McDowell, "The TREAT Upgrade Manual Reactor Control System and Its Interface with the Automatic Reactor Control System and the Plant Protection System," **IEEE Tran. Nucl. Sci., 33,** 703 (1986).

[4] J. A. Bernard and D. D. Lanning, "Issues in the Closed-Loop Digital Control of Reactor Power: The MIT Experience," **IEEE Tran. Nucl. Sci., 33,** 992 (1986).

[5] S. E. Binney and A. J.M. Bakir, "Design and Development of A Personal-Computer-Based Reactivity Meter for a Research Reactor," **Nucl. Technol., 85,** 12 (1989).

[6] J. A. Bernard, A. F. Henry, and D. D. Lanning, "Application of the Reactivity Constraint Approach to Automatic Reactor Control", **Nucl. Sci. Eng., 98,** 87 (1988).

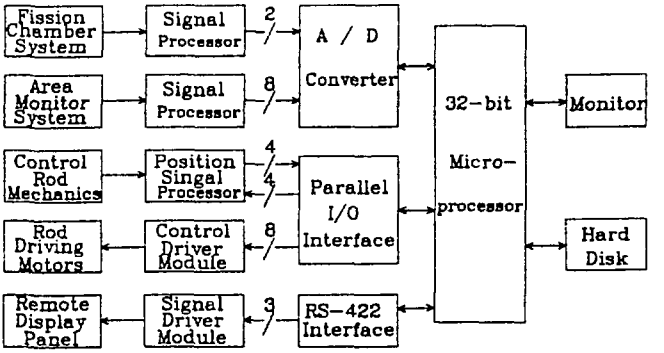

Figure 1 Block diagram of the monitoring and control system.

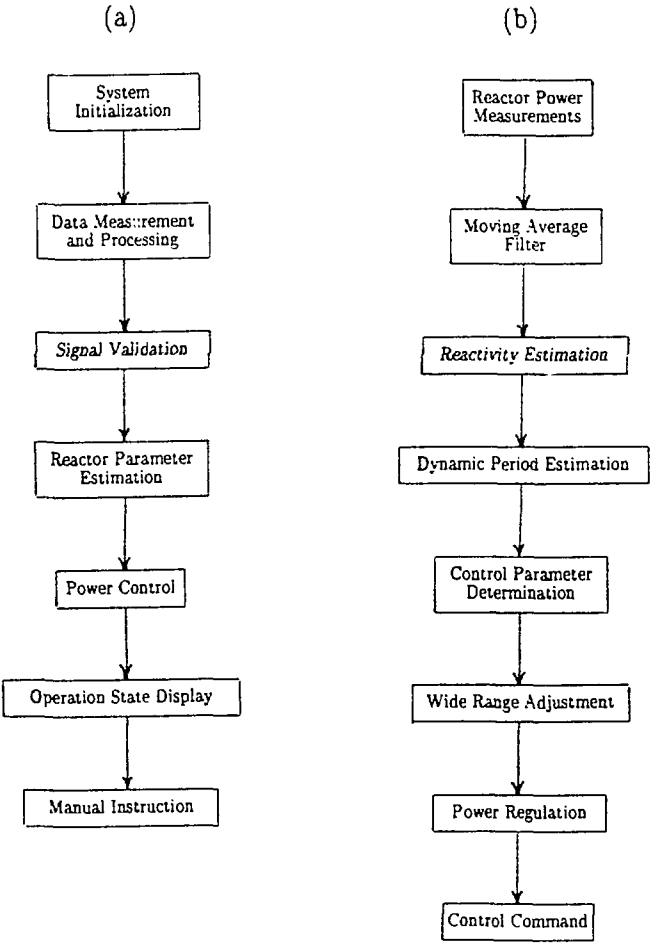

Figure 2 (a) Flow chart of the monitoring and control system;
(b) Flow chart of the power control scheme.

(a)

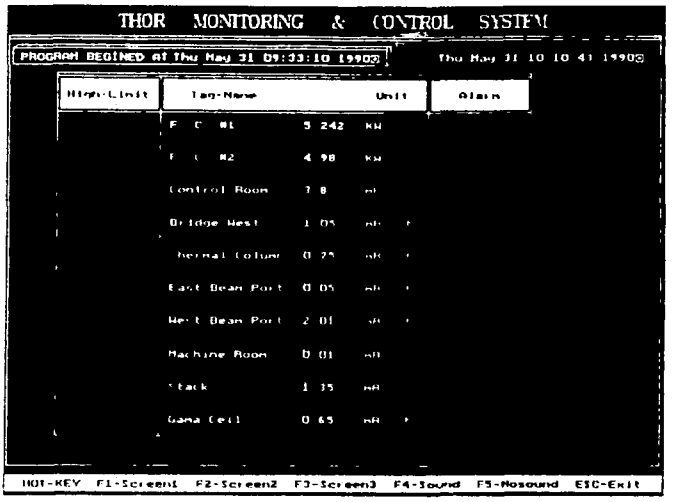

(b)

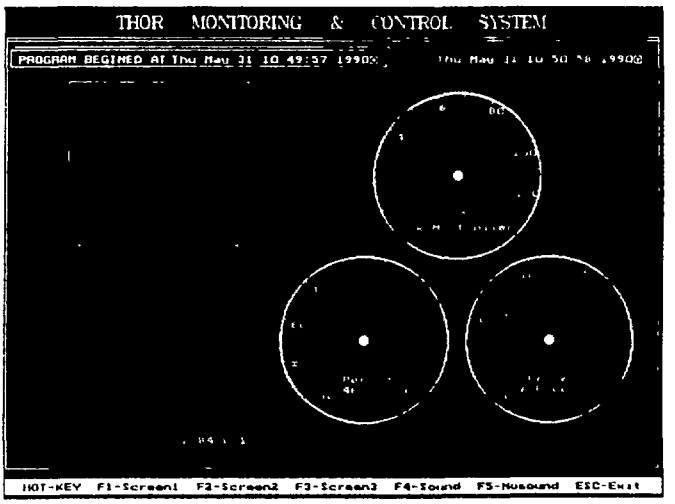

(c)

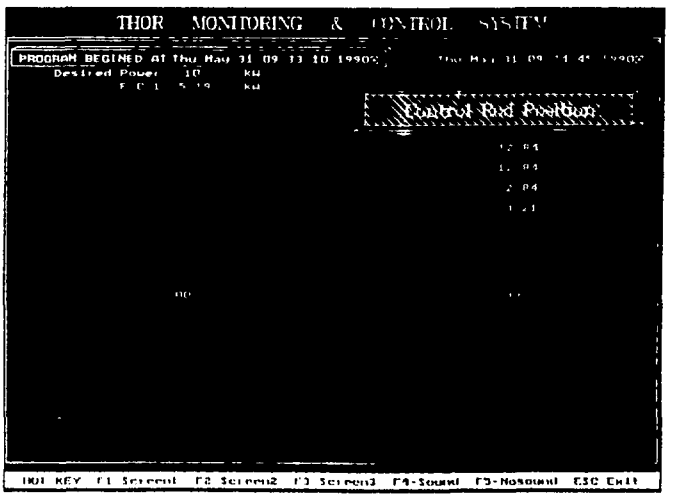

Figure 3 (a) Power and radiation level display; (b) Display of a simplified instrumentation panel; (c) Diplay of history of parameters.

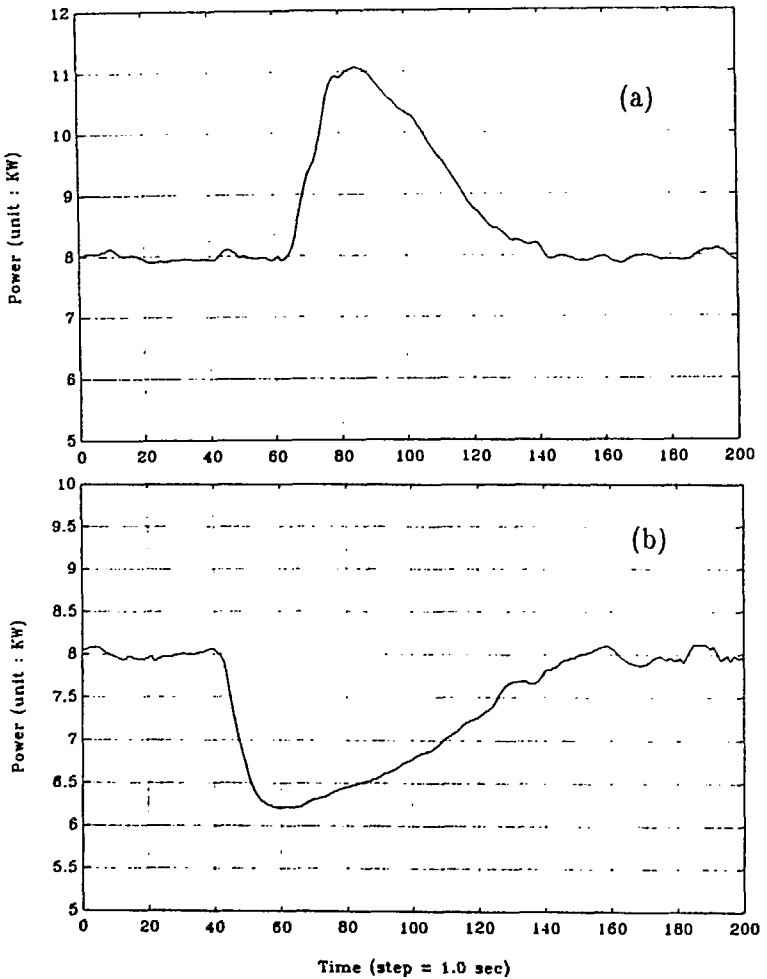

Figure 4 Disturbance rejection tests with a control blade (a) suddenly withdrawl and (b) suddenly insertion.

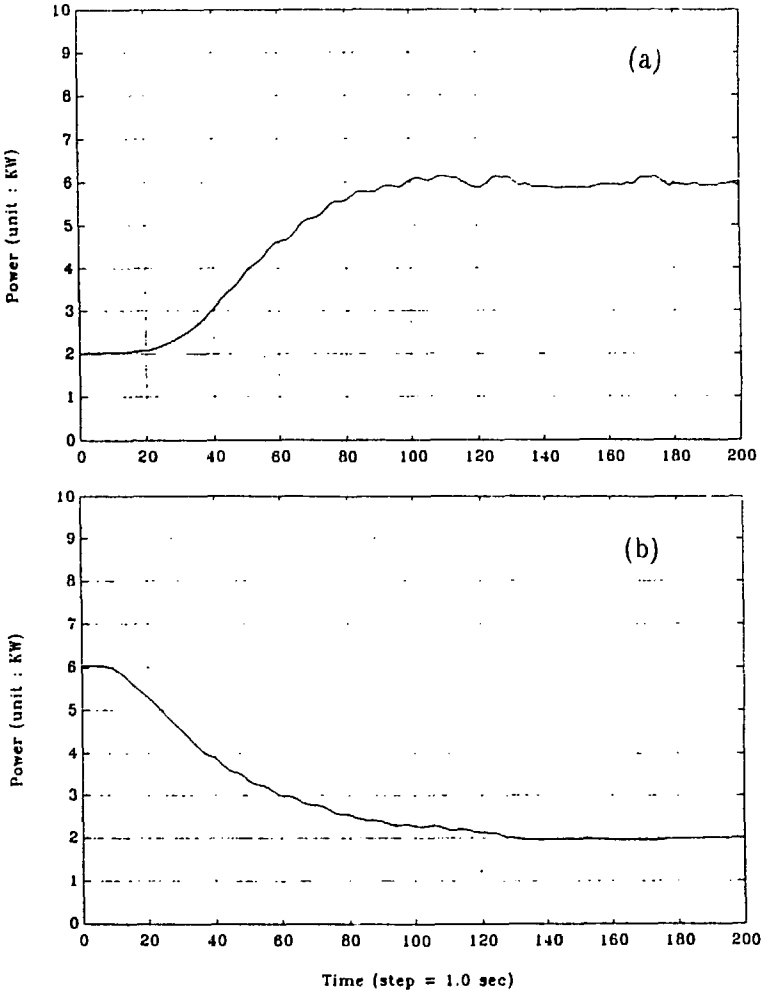

Figure 5 Power adujustment via automatic control (a) power increment and (b) power reduction.